ASSOCIAÇÃO BRASILEIRA DE ENERGIA NUCLEAR - ABEN
2019 International Nuclear Atlantic Conference - INAC 2019
Santos, SP, Brazil, October 21-25, 2019

Agência Brasileira do ISBN
ISBN 978-85-99141-08-3
9 788599 141083

A DIFFRACTOMETER PROJECT FOR BRAZILIAN MULTIPURPOSE REACTOR (RMB): MCSTAS SIMULATIONS AND INSTRUMENT OPTIMIZATION

Alexandre P. S. Souza[1], Luiz P. de Oliveira[1], Fabiano Yokaichiya[2], Frederico A. Genezini[1], Margareth K. K. D. Franco[1]

[1]Instituto de Pesquisas Energéticas e Nucleares (IPEN/CNEN)
Reator Multipropósito Brasileiro (RMB)
Av. Professor Lineu Prestes 2242
05508-000 São Paulo, SP
alexandre.souza@ipen.br

[2]Helmholtz-Zentrum Berlin für Materialien und Energie
Department Quantum Phenomena in Novel Materials
Hahn-Meitner-Platz 1
14109 Berlin, Alemanha
fabiano.yokaichiya@gmail.com

ABSTRACT

High-resolution diffractometer is one of the first instruments of the set of 15 priority neutron scattering instruments to be installed at the Brazilian Multipurpose Reactor (RMB). A basic project of this instrument consists of the existence of three guides through which neutrons pass from source to sample to guarantee maximum neutron flux at the sample position. In this study we investigate guide geometry performance considering fixed diffractometer geometry and spatial arrangement. Comparisons between different guide shapes and supermirrors are performed using software based on the Monte Carlo method, McStas. Our conclusion shows that a better solution is splitting the initial flux into two different guides to obtain the maximum flux at the sample position.

1. INTRODUCTION

The upcoming Brazilian Multipurpose Reactor (RMB) is a new facility designed for radioisotope production and neutron-beam research [1]. The diffraction technique is very important and well established for our understanding of solid state of matter and consequently is one of the priorities of RMB instruments. There are some advantages to studying structures at the atomic scale with neutrons. They are particles that have spin $^1/_2$ and no electric charge. Thus, their interactions mainly occur with other atom nuclei instead of electrons as in X-ray interaction. In addition, properties allow investigating magnetic structures in the matter and light elements in the presence of heavy ones.

Neutron instruments are generally expensive and require a previous study of components and performance before being installed or build. In this spirit, McStas software is an available tool frequently used to simulate neutron instruments for reactors and spallation facilities [2]. It provides components to construct virtual instruments and it uses the Monte Carlo method to produce neutron beams to verify their performance.

Once RMB has in OPAL its reference reactor, we consider it plausible to use a powder diffractometer of this facility, called ECHIDNA, as a first approach of the project. According to literature, and ECHIDNA available information, we build a basic diffractometer that mimics OPAL's instrument [3, 4]. However, we adapt such instrument to other sources by using McStas components `Source_gen()` and `Virtual_mcnp_input()` [5]. We compare results from ILL (thermal) source produced by `Source_gen()` with IEA-R1 source read by `Virtual_mcnp_input()`. The latter source was created by MCNP simulations of IEA-R1 Brazilian reactor at Instituto de Pesquisas Energéticas e Nucleares - IPEN.

The way to connect any source to an instrument is crucial to better utilize available flux that arrives at the sample position and consequently at the detector. In OPAL, for instance, the flux that reaches the ECHIDNA monochromator comes from WOMBAT High-intensity diffractometer [4]. Then, the uses and delivering definition of available neutron flux (neutron guides definition) to any instrument is important to avoid losing and optimize its uses.

In this study, we intend to investigate those guide configurations that provide maximum flux at the sample position. We focus on simulating a basic diffractometer configuration inspired on ECHIDNA with different neutron guide systems (different guide length and supermirrors) in order to identify advantageous scenarios. In the next section, we describe diffraction technique, McStas simulations and virtual diffractometer components. The last section contains the final remarks and conclusions.

2. DIFFRACTION TECHNIQUE AND MCSTAS SIMULATIONS

The powder high-resolution diffractometer combined with the Rietveld refinement method is applied in distinguishing different Bragg peaks, which is necessary for material structure and sample phases determination [6, 7]. In such a scenario, any optimization consists of increasing resolution with no expense of intensity. There are a lot of studies in the literature that discuss many aspects of diffractometer in order to achieve fine resolution without losing intensity or to try to increase intensity in real facilities high-resolution instruments [8, 9, 10, 11].

The paper of Caglioti and collaborators is a milestone in diffractometer setting and optimization [12]. Consequently, current instrument optimizations have in Caglioti's assembly the first step to obtain a fine resolution. In short, almost all modifications in components of the Caglioti diffractometer are based on instrument geometry and the use of horizontal or vertical focusing monochromator. Vertical focusing is an example of a process that allows a gain factor between 2 and 10 at the sample position with no change in instrument resolution [13].

However, before analyzing collimator and monochromator properties it is necessary to guarantee a maximum flux delivery to sample position. Consequently, we decide to first ensure guide system efficiency before studying instrument optimization like geometry, components and samples.

Diffractometer configuration is shown in Figure 1. Transportation components of simulations consist of a funnel guide, a main guide and a second guide that is between monochromator and sample position. Other McStas components form a simple version of the ECHIDNA high-resolution diffractometer. Such an instrument has a vertical focusing monochromator [3, 4]. Collimation is provided by a primary Soller collimator, a secondary Soller collimator, a radial collimator, which follows the Caglioti fundamental configuration [12, 14].

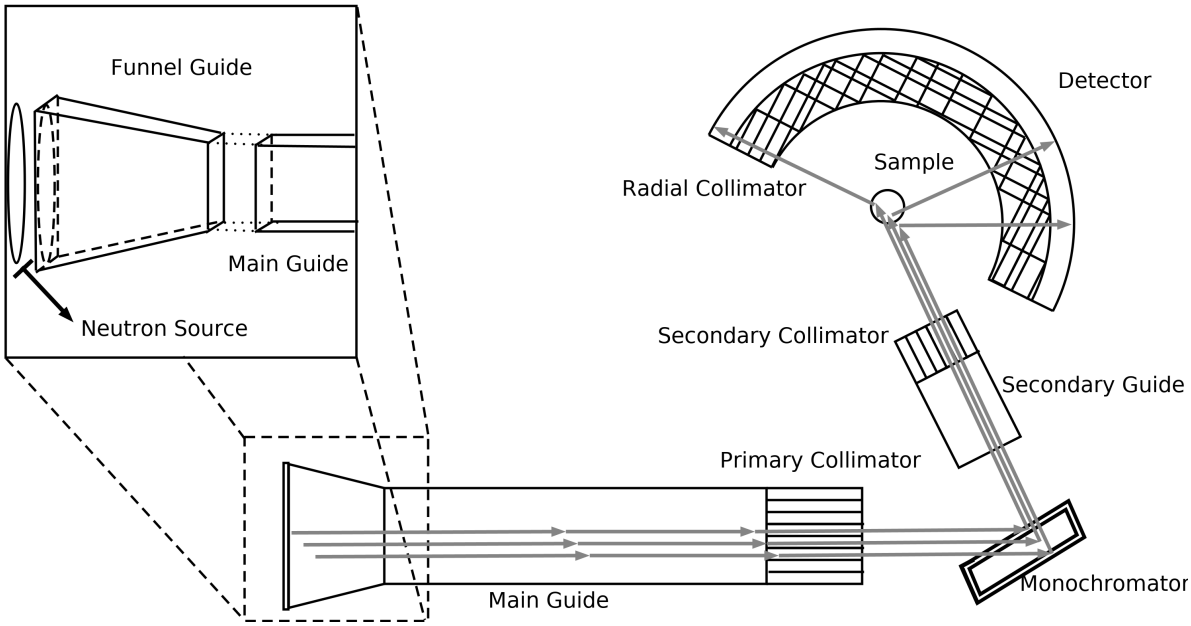

Figure 1: A top-view sketch of simulated diffractometer with a close spotlight on both guide connection.

Input values of McStas simulation components are described in Tables 1 and 2. In Table 1, we present fixed values of monochromator height (h) and mosaicity (β), takeoff angle (θ_M), reflected wavelength (λ) and collimation (α_1, α_2 and α_3), where such values correspond to real parameters of ECHIDNA high-resolution diffractometer [4]. Table 2 constains simulation cases for different funnel and main guides length (L_{FG} and L_{MG}, respectively) and supermirrors (m value, where $m\theta_c^{Ni}$ is the critical angle of supermirror and θ_c^{Ni} is the critical angle of reflection of Ni^{58}). It is worth noting that values of guide length already include collimator length, namely 70 cm for primary collimator and 30 cm for secondary collimator.

The IEA-R1 source, which has been produced with MCNP code, mimics the real flux of the Brazilian reactor. According to this data and reactor geometry, the beam hole aperture, where neutrons are being produced, has a radius of about 8.5 cm. In addition, we adopt the same thermal guide dimensions of TG1, where ECHIDNA is located at OPAL, for our simulations. Thus, the main guide has 5 cm width and 30 cm height with the variable length depending on the simulation case, as described in Table 2. Since source area (16.8×16.8 cm^2) is larger than guide entrance (30×5 cm^2), we propose a funnel guide to concentrate neutron flux into the main guide in an attempt to use all available neutrons. In this assembly, funnel guides are designed to have 16.8 cm width and 16.8 cm height at the guide entry and 5 cm width and 30 cm height at the guide exit, where it

Table 1: Simulation technical data of diffractometer

Components and Instrument Characteristics	Adopted Values
Monochromator	23 slabs $\beta = 33'$ $h = 300$mm
Takeoff Angle	$\theta_M = 140^o$
Wavelength	$\lambda = 1.62$Å
Collimation	$\alpha_1 = 10'$ $\alpha_2 = 10'$ $\alpha_3 = 5'$

connects itself with the main guide, as shown in Figure 1.

Divergence of neutron source and supermirrors are important to determine the fraction of initial flux that reaches the sample. Besides, simulation results of Table 2 allow us to define guides. Within such results, we are able to decide if it is worth to split source flux between two or three guides to supply neutron flux for different instruments or to keep just a single guide to feed one or two instruments (like in TG1 at OPAL). Gilles *et al.* found that a secondary guide between monochromator and sample position deteriorate profile quality [15]. Here we also propose to check if this secondary guide is important to keep flux at the sample position. Simulations 1 and 2 in Table 2 correspond to cases with no guides ($\varnothing$) and distance of 8 m between source and primary collimator.

The simulated monochromator was constructed based on literature, where a vertical focusing monochromator is provided by a curved assembly of monocrystal wafers also known as a finger. Its curvature is linked to diffractometer geometry by the following equation:

$$\frac{1}{R_v} = \frac{1}{2\sin\theta_M}\left(\frac{1}{L_1} + \frac{1}{L_2}\right), \tag{1}$$

where R_v is monochromator curvature radius, θ_M is takeoff angle, $L_1 = L_{FG} + L_{MG}$ and L_2 is monochromator-sample distance [16]. Following this relation, we ensure maximum flux at the sample position. However, there are in literature other ways to maximize incoming flux in the curved detector besides monochromator vertical focusing. Horizontal focusing monochromator and sample size adjustment are available possibilities, which are let to be analyzed in detail in future studies.

We have placed four detectors between the main components of the diffractometer in order to study flux behavior. They are between source and guide entrance, primary collimator and monochromator, monochromator and secondary guide entrance and between secondary collimator and sample position. All data of such detector are presented in four columns in both result Tables. Namely F_S, F_{C1}, F_M and F_{C2}. All simulations presented in Table 2 were carried out and flux values were verified. Their results are shown in Table 3 for IEA-R1 source and in Table 4 for ILL.

Table 2: McStas Simulation Cases.

Simulation	**Source**	L_{FG}(m)	L_{MG}(m)	m
1	IEA-R1	∅	∅	∅
2	ILL	∅	∅	∅
3	IEA-R1	58	0	0
4	IEA-R1	58	0	1
5	IEA-R1	58	0	2
6	IEA-R1	58	0	3
7	ILL	58	0	0
8	ILL	58	0	1
9	ILL	58	0	2
10	ILL	58	0	3
11	IEA-R1	0	58	0
12	IEA-R1	0	58	1
13	IEA-R1	0	58	2
14	IEA-R1	0	58	3
15	ILL	0	58	0
16	ILL	0	58	1
17	ILL	0	58	2
18	ILL	0	58	3
19	IEA-R1	3	55	2
20	ILL	3	55	2
21	IEA-R1	3	5	2
22	ILL	3	5	2
23	IEA-R1	5	5	2
24	ILL	5	5	2
25	IEA-R1	10	5	2
26	ILL	10	5	2
27	IEA-R1	15	5	2
28	ILL	15	5	2

Table 3: Simulation Results with IEA-R1 Source

Source:		**IEA-R1**			
Simulation	**Neutron Flux Detection**				
	Detector Position:	**Source**	**Primary Collimator**	**Monochromator**	**Secondary Collimator (Sample)**
	Detector Area (cm^2):	16.8 × 16.8	30 × 5	30 × 5	12.8 × 5
	m	F_S ($\times 10^{11} n/cm^2 s$)	F_{C1} ($\times 10^{7} n/cm^2 s$)	F_M ($\times 10^{6} n/cm^2 s$)	F_{C2} ($\times 10^{6} n/cm^2 s$)
1	∅	2.504	40.75	34.10	30.57
3	0	2.504	6.912	1.628	2.536
4	1	2.504	9.766	1.731	2.677
5	2	2.504	13.89	1.792	2.747
6	3	2.504	16.19	1.834	2.715
11	0	2.504	7.034	1.752	2.860
12	1	2.504	8.675	1.078	2.306
13	2	2.504	12.54	1.132	2.133
14	3	2.504	16.05	1.138	2.131
19	2	2.504	12.67	1.165	2.211
21	2	2.504	39.99	31.54	27.96
23	2	2.504	34.08	24.44	23.36
25	2	2.504	27.78	22.55	19.62
27	2	2.504	23.73	18.20	17.76

Table 4: Simulation Results with ILL Source

Source:		**ILL**			
Simulation	**Neutron Flux Detection**				
	Detector Position:	**Source**	**Primary Collimator**	**Monochromator**	**Secondary Collimator (Sample)**
	Detector Area (cm^2):	16.8 × 16.8	30 × 5	30 × 5	12.8 × 5
	m	F_S ($\times 10^8 n/cm^2 s$)	F_{C1} ($\times 10^7 n/cm^2 s$)	F_M ($\times 10^5 n/cm^2 s$)	F_{C2} ($\times 10^4 n/cm^2 s$)
2	∅	133.0	115.7	32.60	111.0
7	0	2.106	9.605	2.491	7.712
8	1	2.107	11.61	3.083	9.791
9	2	2.108	11.67	3.216	10.98
10	3	2.107	11.67	3.223	10.91
15	0	2.159	9.258	2.554	8.512
16	1	2.159	10.84	2.942	10.01
17	2	2.158	11.02	2.994	10.13
18	3	2.159	11.02	3.050	9.489
20	2	786.4	50.83	11.68	37.90
22	2	786.3	180.2	51.25	169.3
24	2	283.4	138.3	37.16	128.6
26	2	70.86	82.66	22.83	75.38
28	2	31.51	55.07	15.25	49.83

Here we focus on comparing flux values of source and primary collimator and also monochromator and sample since monochromator parameters were fixed during simulations. After comparing fluxes of source (first column) and primary collimator (second column) for different supermirrors in Table 3, we observe, as expected, a continuous increase of incoming flux at monochromator according to m values (from $m = 0$ to $m = 3$).

We verify cases where there is an enhance in flux between monochromator and sample due to monochromator focusing. In other words, the neutron stream is passing throw a smaller area in the sample position than in the monochromator without losing many neutrons. According to results (last column of Tables 3 and 4) and considering that the monochromator area is about 60% larger than detector area at the sample position, it is possible to guarantee that there are no significant neutron flux loss corresponding to secondary guide. In Table 3 the minimum loss is about 10% (simulation 12) and maximum about 60% (simulation 27).

There is another interesting result in Table 3. By checking simulations 1 and 21 we observe that both fluxes after primary collimator are compatible. This happens because distances with and without guides are equivalent (8 m). This result shows, at least for this diffractometer assembly, that for short distances the use of the guide is not crucial. This justifies the use of beam tubes instead of neutron guides in facilities where thermal neutron instruments are located near to reactor face like in HZB, for instance. In this context, we observe the same behavior in monochromator and secondary collimator flux comparison, which is coherent to Gilles *et. al.* study[15].

We believe that this behavior is due to an internal characteristic of McStas component `Source_gen()`, which is used to produce ILL source. It is a virtual source with distance to target along the z-axis as simulation input [17]. In our simulations, such distance was adopted to correspond to source-primary collimator distance in a way that neutrons have no divergence enough to hit guide walls. That is the reason for finding no significant variation on F_{C1} in cases 8, 9 and 10, and 16, 17 and 18 of Table 4. In these terms, define properly this distance of aim is crucial for using these virtual sources to mimic real ones.

By comparing fluxes after primary collimator (of column F_{C1}) of simulation 3 to 6 with 11 to 14 of Table 3 and also simulation 7 to 10 with 15 to 18 of Table 4, we confirm that the use of funnel guide is not significant in flux gain. Consequently, a better way to use available neutrons is, at least to this scenario, to split the main neutron source area into two instruments. Another possible way to "save" neutron flux is by using transmitted upstream of monochromator as well as WOMBAT and ECHIDNA diffractometer at OPAL [4].

3. CONCLUSIONS

We verify a weak dependence on supermirror variety (m) in ILL results. In this study, we propose a basic assembly of a high-resolution powder diffractometer to be installed at RMB. OPAL's correspondent diffractometer ECHIDNA is taken as a very first project configuration. Initial simulations were carried out to investigate neutron flux of this basic diffractometer. We analyze flux at four different parts of the instrument stream to compare guides performance. Initial results show that there is just a subtle variance of flux for the instrument close to the face reactor (about 8 m). According to our results, we also verified that the secondary guide between monochromator and sample position is not necessary for this diffractometer configuration.

We also find that the funnel guide should be long enough to diminish the flux divergence, but results with long funnel guides (58 m) do not show significant variation next to normal straight guides (main guide) with the same length. In these terms, a better solution would be splitting initial flux in two different guides instead of using a funnel guide to focus and "save" neutrons from a source with a larger area than the main guide. Availing transmission neutron flux of monochromator in the same way as OPAL's WOMBAT and ECHIDNA instruments is also a possibility to maximize neutron use.

ACKNOWLEDGMENTS

APSS and LPO would like to thank CNPq for financial support under grant numbers 381565/2018-1 and 380183/2019-6, respectively, as well as FAPESP for financial support at INAC 2019. We would like to thank Dr. Paulo De Tarso Dalledone Siqueira at CEN/IPEN, for the IEAR-1 source file and discuss on MCNP code.

REFERENCES

1. J. A. Perrotta, A. J. Soares, F. A. Genezini, F. A. Souza, M. K. K. D. Franco, and E. Granado, "Future perspectives for neutron beam utilization in brazil," *Neutron News*, **25**, no. 4, pp. 3–5, (2014).
2. K. Lefmann and K. Nielsen, "Mcstas, a general software package for neutron ray-tracing simulations," *Neutron News*, **10 (3)**, pp. 20 – 23, (1999).
3. K.-D. Liss, B. Hunter, M. Hagen, T. Noakes, and S. Kennedy, "Echidnathe new high-resolution powder diffractometer being built at opal," *Physica B: Condensed Matter*, **385-386**, pp. 1010 – 1012, (2006).
4. M. Avdeev and J. R. Hester, "ECHIDNA: a decade of high-resolution neutron powder diffraction at OPAL," *Journal of Applied Crystallography*, **51**, pp. 1597–1604(Dec, 2018).
5. "Components and instruments from the library for *McStas*." `http://www.mcstas.org/download/components/`. Accessed: 27/06/2019.
6. H. M. Rietveld, "A profile refinement method for nuclear and magnetic structures," *Journal of Applied Crystallography*, **2**, pp. 65–71(Jun, 1969).
7. H. M. Rietveld, "The rietveld method," *Physica Scripta*, **89**, p. 098002(aug, 2014).

8. A. Buchsteiner and N. Ster, "Optimizations in angular dispersive neutron powder diffraction using divergent beam geometries," *Nuclear Instruments and Methods in Physics Research Section A: Accelerators, Spectrometers, Detectors and Associated Equipment*, **598**, no. 2, pp. 534 – 541, (2009).
9. M. Hoelzel, A. Senyshyn, N. Juenke, H. Boysen, W. Schmahl, and H. Fuess, "High-resolution neutron powder diffractometer spodi at research reactor frm ii," *Nuclear Instruments and Methods in Physics Research Section A: Accelerators, Spectrometers, Detectors and Associated Equipment*, **667**, pp. 32 – 37, (2012).
10. L. van Eijck, L. D. Cussen, G. J. Sykora, E. M. Schooneveld, N. J. Rhodes, A. A. van Well, and C. Pappas, "Design and performance of a novel neutron powder diffractometer: PEARL at TU Delft," *Journal of Applied Crystallography*, **49**, pp. 1398–1401(Oct, 2016).
11. J. Zhang, Y. Xia, Y. Zhang, B. Pang, G. Sun, J. Li, C. Huang, Y. Wang, J. Pan, and C. Xie, "Performance improvement of the high resolution neutron diffractometer at CAEP with geant4 simulation," *Journal of Instrumentation*, **12**, pp. P10007–P10007(oct, 2017).
12. G. Caglioti, A. Paoletti, and F. Ricci, "Choice of collimators for a crystal spectrometer for neutron diffraction," *Nuclear Instruments*, **3**, no. 4, pp. 223 – 228, (1958).
13. P. Courtois, "Vertical neutron beam focusing with bent mosaic crystals," *Journal of Physics: Conference Series*, **746**, p. 012005(sep, 2016).
14. A. Hewat, "Design for a conventional high-resolution neutron powder diffractometer," *Nuclear Instruments and Methods*, **127**, no. 3, pp. 361 – 370, (1975).
15. R. Gilles, G. Artus, J. Saroun, H. Boysen, and H. Fuess, "The new structure powder diffractometer at the frm-ii in garching," *Physica B: Condensed Matter*, **276-278**, pp. 87 – 88, (2000).
16. R. Lechner, R. v. Wallpach, H. Graf, F.-J. Kasper, and L. Mokrani, "A monochromator with variable horizontal and vertical curvatures for focussing in real and reciprocal space," *Nuclear Instruments and Methods in Physics Research Section A: Accelerators, Spectrometers, Detectors and Associated Equipment*, **338**, no. 1, pp. 65 – 70, (1994).
17. "The `source_gen` component." `http://www.mcstas.org/download/components/sources/Source_gen.html`. Accessed: 27/06/2019.